



### Research Article

## Performing reactive power compensation of three-phase induction motor by using parallel active power filter

Ömer Ali Karaman <sup>a</sup> , Ahmet Gündoğdu <sup>b,\*</sup>  and Mehmet Cebeci <sup>c</sup> 

<sup>a</sup>Batman University, Department of Electric, Vocational School, Batman, 72000, Turkey

<sup>b</sup>Batman University, Department of Electrical and Electronic Engineering, Batman, 72000, Turkey

<sup>c</sup>Firat University, Department of Electrical and Electronic Engineering, Elazığ, 23000, Turkey

#### ARTICLE INFO

##### Article history:

Received 03 May 2020

Revised 11 June 2020

Accepted 05 July 2020

##### Keywords:

Harmonics

Parallel active power filter

Power factor correction

3-phase induction motor

#### ABSTRACT

Nowadays, the problem of power quality increases day by day. Harmonic current and reactive power are the important factors disturbing the power quality. The induction motors draw both harmonic current and reactive power from the grid. Reactive power and harmonic current lead to heat losses and decrease in the efficiency of the transmission lines. Passive and active filter applications have been used to solve these problems. There are some disadvantages of passive filters. Large physical dimensions and resonance with load can be shown as examples for these disadvantages. Therefore, the application areas of Active Power Filter (APF) are rapidly developing due to the fact that they can be applied together with harmonic and reactive power compensation as appropriate control methods. This paper proposes a MATLAB/Simulink simulation to perform power factor correction and reactive power compensation of three-phase induction motor by using three-phase Parallel Active Power Filter (PAPF). In order to generate PAPF's reference currents the Sine Multiplication Technique (SMT) is used. Simulation studies are presented to be able to assess the performances under different motor operating conditions. The proposed hysteresis controller based PAPF filter makes the power factor up to 1 and the reactive power compensation of the three-phase induction motor.

© 2020, Advanced Researches and Engineering Journal (IAREJ) and the Author(s).

### 1. Introduction

Induction motors are widely utilized in many different applications [1]. An important percentage of the energy generated in an industrialized country is consumed by induction motors [2]. However, the main disadvantages of them are that they require reactive power and draw harmonic currents. Reactive power leads to heat losses and decrease in the efficiency of the power systems. To reduce or solve many of the problems related to the power quality, the optimal control of the reactive power can be applied [3]. It is also possible to make significant financial saving with the reactive power compensation. The circulation of reactive power in the grid in a system without reactive power compensation is shown in Figure1.

In terms of controlling power systems, one of the important problems is reactive power compensation. In the power systems, to increase the current carrying

capacity and to reduce the size of the transmission line conductor, reactive power compensation is required. Thus, it leads to the reduction of losses. Also, the production cost of the transmission system is reduced [4]. There are many advantages of producing reactive power at the point close to the load and giving it to the grid in order to prevent excessive current circulation caused by the reactive power requirement in the grid. This application is known as the conventional reactive power compensation method. It is also called "power factor correction". Figure2 shows the reactive power circulation in the grid after the compensation is performed.

Therefore, the reactive power should be reduced by correcting the power factor. Passive filter applications have long been used to solve these problems. Nevertheless, it is possible to mention many disadvantages of passive filters, such as settling to certain frequency values, resonance with load, and large physical

\* Corresponding author. Tel.: +90 488 217 41 06.

E-mail addresses: [omer.ali.karaman@batman.edu.tr](mailto:omer.ali.karaman@batman.edu.tr) (Ö.A. Karaman), [ahmet.gundogdu@batman.edu.tr](mailto:ahmet.gundogdu@batman.edu.tr) (A. Gündoğdu), [mcebeci@firat.edu.tr](mailto:mcebeci@firat.edu.tr) (M.Cebeci)

ORCID: 0000-0003-1640-861X (Ö.A. Karaman), 0000-0002-8333-3083 (A.Gündoğdu), 0000-0002-2971-6788 (M.Cebeci)

DOI: 10.35860/iarej.731187

dimensions. Because conventional compensation systems can not immediately respond to the reactive power demand that a load needs in a moment, correcting the loads' power factor, which is powerful and has the ability to enter and leave the circuit swiftly, cannot be achieved by applying the conventional electromechanical compensation arrangements. The rapid increase in technology has also increased the importance of compensation realized by using modern methods.

When the compensation of power systems is done with semiconductor switches, the voltage collapses can be avoided and it can improve transient and dynamic stability [5,6]. Besides, reactive power compensation should be used to reduce current harmonics [7]. In electrical systems, nonlinear loads draw nonlinear current from the grid. In power systems, voltage harmonics are generated by nonlinear currents. Then, all system elements are affected by spreading of these voltage harmonics to the entire power system. Due to current and voltage harmonics, overheating of transformers, increasing of losses, reduction in the power factor, and decreasing of the system efficiency are experienced [8]. In terms of the Point of Common Connection (PCC), there are some limitations brought by the IEEE Standards 519 to the voltage and current harmonics. The above-mentioned standards recommend that the determined value of the Total Harmonic Distortion (THD %) should be 3% for the voltage and 5% for the current. Because the power systems' receivers are affected negatively by harmonic currents, these standards have been prepared to ensure that the harmonic currents are kept within the determined limits [9].

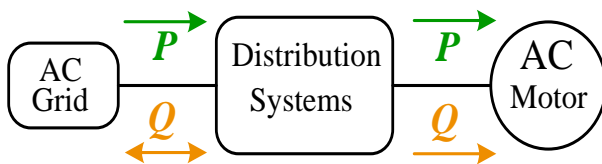


Figure 1. Reactive power circulation in the grid.

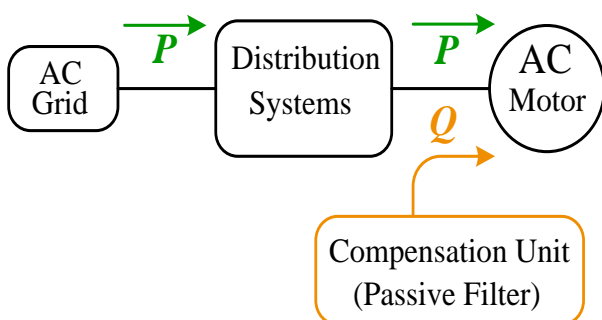


Figure 2. Conventional compensation system

Active power filters (APF) are called devices that both compensate and eliminate harmonics by using semiconductor switches. Due to the switching capabilities of the power switches at very high frequencies, active power filters can also filter high frequency current and voltage harmonics, perform reactive power compensation, reduce neutral line currents and eliminate imbalance emerging in three-phase systems.

Nowadays, various active power filters (e.g., serial, parallel, hybrid and combined power quality regulators) are used to find solutions for power quality problems. The most common and widely utilized active power filter method in the industry is the parallel active power filter (PAPF) [10,11].

For example, in distribution systems, to be able to ensure the optimal reactive power compensation, an optimal phase angle model and allocation method of multiple Distribution-STATCOM (DSTATCOM) was proposed. The proposed method is more influential in compensation of the reactive power for the reduction of the power loss [12].

One of the effective methods of performing reactive power compensation in industrial applications is the hybrid active power filter because it allows low-cost high power applications [13].

For different compensations in a system that had static and dynamic loads, a 3-phase DSTATCOM was applied and its performance analysis was carried out. In this study, to generate the reference signal, the synchronous reference frame theory was used and the hysteresis pulse width modulation switching was applied for the firing pulse generation, and these were realized in the field-programmable gate array (FPGA) [14].

A model to correct the power factor, and digital implementation of various loops of a circuit (e.g., hysteresis controller for current loop and PI controller for voltage loop) were presented. Fixed, sinusoidal and variable bands were implemented and they were verified through simulation. Compared to other hysteresis control methods, the variable band hysteresis control gave lower THD value for the input current in the current loop [15]. For the shunt active power filter depending on the predictive direct power control through the space vector modulation, a powerful control design was proposed. The problem of the variable switching frequency of the predictive control method was solved by the proposed design, and it offered simple and powerful hardware application [16]. Instead of conventional compensation systems, PAPF ensures dynamic and rapid reactive power compensation even under very changeable load conditions [17].

A simple controller structure with minimal feedback that ensured the open-ended winding induction motor (OEWM), used in the Dual inverter drive (DID) system,

to operate under constant power factor under different load and speed conditions was proposed [18].

Reactive power compensation of an induction motor with nine switching elements and fed through an AC-DC-AC converter was performed. A PI controller was developed to achieve the desired power factor within the closed-loop control structure [19].

The effects of the active power filter (APF) on power quality at the output of a synchronous generator with a distorted back-EMF waveform were examined. In simulation and experimental studies conducted using APF, it was observed that THD was significantly reduced [20].

A new adaptive fuzzy-based hysteresis current control technique was proposed to reduce current harmonics and switching losses in a system using the hybrid active power filter (HAPF). Experimental studies showed that switching losses were reduced by 9% [21].

In addition to having a fast dynamic response, the “bipolar hysteresis current control technique” used in two-stage photovoltaic (PV) micro-inverters has high efficiency even at high switching frequencies. To reduce switching losses at high switching frequencies, the unipolar hysteresis current control technique is preferred. However, in also this control technique, zero-crossing distortions and low-frequency harmonics occur in the grid current. To solve this problem, the technique of proportional resonant (PR) and hybrid hysteresis current control was proposed [22].

Electric motors and other inductive loads need reactive power. They draw the power they need either from the grid or from fixed-capacity compensation units called passive filters. The active power filters developed as an

alternative system both meet the reactive power requirement of the system and make the power factor of the system one (1) at each load stage. In the literature, there are different studies on the reactive power compensation of parallel active power filter (PAPF) and 3-phase induction motor. However, studies that SMT, which is the reference current prediction technique, and HBCC, which is the hysteresis controller structure, are used together has not been encountered. In order to contribute to this area, a model in which the Sine Multiplication Technique (SMT) and Hysteresis Band Current Controller (HBCC) structure were used together was created. With this model created in MATLAB/Simulink environment, reactive power compensation of a 3-phase induction motor was performed. With simulation studies for no-load and loaded operating conditions, the power factor of the system was successfully increased to 1. In this respect, this study is different from other studies that have been conducted and it partly contains originality.

## 2. Entire System and Proposed Filter

As seen in Figure 3, the system simulation consists of three-phase induction motor, the sine multiplication technique control block to determine the reference current, dc-link capacitor, 3-wired two-level voltage source inverter, hysteresis band current controller (HBCC), and a coupling inductance to connect the inverter to the grid.

Although the literature includes a lot of complex control algorithms, the use of the simple structure hysteresis controller with the Sine Multiplication Technique has the advantages of being easy-applicable and easy to perform with low speed microprocessors.

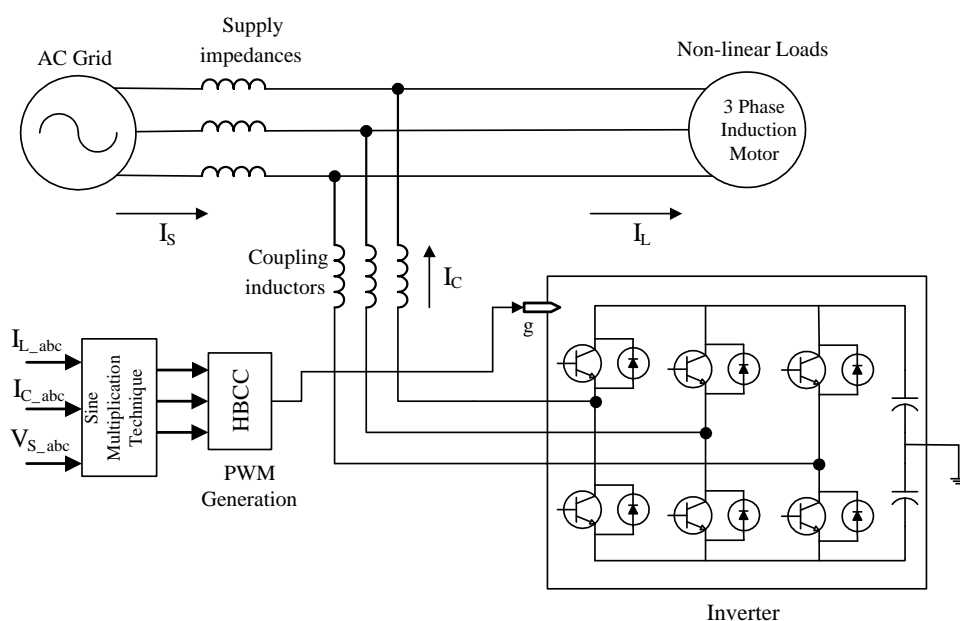


Figure 3. Block diagram of the PAPF

**2.1 Parallel Active Power Filter (PAPF)**

Among the active power filters, the one that is the most commonly utilized in the industry is the parallel active power filter [23]. Figure 4 shows the general structure of the PAPF's voltage source [26]. A PAPF consist of an inverter, a DC link capacitor, a connection inductance that provides connection to the grid and a controller unit. The inverter generates the compensation current. The duty of the connection inductance used on the AC side of the inverter is to prevent the switching parasites generated by the inverter, and the switching signals for the inverter are generated by the controller.

Injecting currents as equal magnitude and in reverse phase to the grid to be able to get rid of load current's harmonics and performing reactive power compensation can be shown as the primary principles of the PAPF. In this way, the harmonics are eliminated and the source currents start to oscillate sinusoidally. For successful application of PAPF, extracting the correct reference current values and generating gate signals are important. Therefore, it is needed to determine the reactive and harmonic components that are drawn by the load currents in order to extract the reference currents. In the literature, there are various techniques for the extraction of reference currents; some of these are shown in Figure 5 [26].

For the extraction of the harmonic current/voltage components in APF practices, a lot of methods that can be performed both in frequency and time domains have been proposed and assessed.

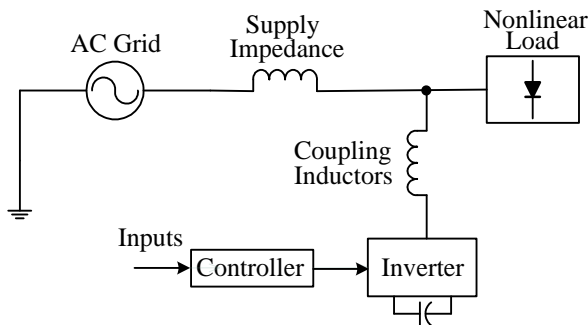


Figure 4. Voltage source PAPF.

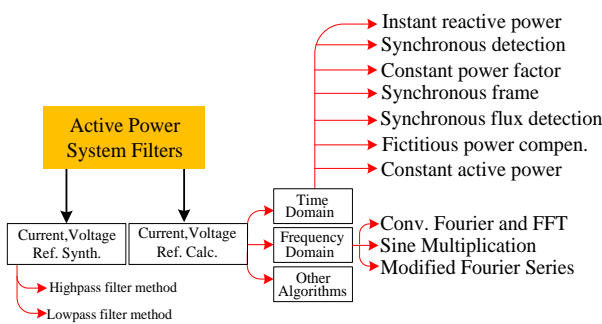


Figure 5. Methods for reference current/voltage extraction

When these methods are examined, it is seen that the most widely used are frequency and time domain based methods [24]. Though there are some distinctive limitations of the techniques used to extract reference current, most of them run stably under fixed loads. Nevertheless, various load circumstances affect their performance significantly. In order to mitigate these effects, different approaches such as Fourier, Artificial Neural Network (ANN) have been proposed in the literature [25,26].

However, these methods presented have some disadvantages. For example, in the method used to extract reference current by depending on the artificial neural networks, a huge amount of data is needed for the training of the network. In this study, for the generation of the active power filter reference currents, the sine multiplication method is used [27].

**2.2 Reference Current Estimation**

The most important part of the PAPF is the reference current extraction part. In this study, the Sine Multiplication Technique was used to find the reference current. SMT is a widely used technique for the determination of the reference compensation currents of PAPFs [28]. However, in power systems where the source voltage is not in ideal sinusoidal form, sine multiplication technique loses effectiveness [27]. Figure 6 shows the block diagram of SMT.

By injecting the predicted reference current into the grid in the opposite phase and with equal amplitude, elimination of the harmonics and realization of the reactive power compensation are achieved. If we assume that the grid is pure (in other words, it does not have harmonics and reactive component), the grid voltage is in the ideal form. Eq. (1) expresses this situation.

$$V_s(t) = V_m \sin \omega t \tag{1}$$

If we assume that a non-linear load is fed by this grid, then the current drawn from the grid can be expressed as shown in Eq. (2).

$$I_L(t) = \sum_{n=1}^{\infty} I_{nm} \sin(n\omega t + \phi_n) = I_{nm} \sin(\omega t + \phi_1) + \sum_{n=2}^{\infty} I_{nm} \sin(n\omega t + \phi_n) \tag{2}$$

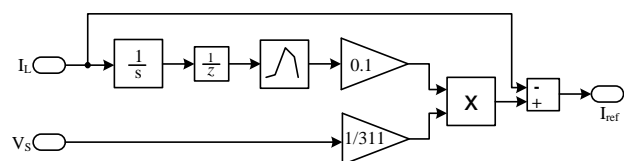


Figure 6. MATLAB/Simulink block diagram of SMT

As seen in the Eq. (2), the fundamental component is the maximum value of the first-order harmonic and  $I_m$  refers to the maximum load current value. Independently from capacitive or inductive load conditions, the sign of the phase angle ( $\varphi_1$ ) of the load is written as a general expression. We can express the instantaneous power that is drawn from the grid as follows;

$$P(t) = V_s(t) \cdot I_L(t) \tag{3}$$

The following power components were obtained by placing Eq. (1) and Eq. (2) in their places at Eq. (3);

$$P(t) = V_m I_m \sin^2 \omega t \cdot \cos \varphi_1 + V_m I_m \cdot \cos \omega t \cdot \sin \omega t \cdot \sin \varphi_1 + V_m \sin \omega t \sum_{n=2}^{\infty} I_{nm} \sin(n\omega t - \varphi_n) \tag{4}$$

It is understood from Eq. (4) that active power as well as infinite number of harmonics and reactive power are drawn from the grid. By separating it from Eq. (4), the active power can be expressed as follows;

$$P_{active} = V_m I_m \cdot \sin^2 \omega t \cdot \cos \varphi_1 \tag{5}$$

As a result of its withdrawal from the active power, the instantaneous power value shown in Eq. (4) and the harmonic and reactive power components are obtained. Reactive power can be shown as;

$$P_{reactive} = V_m I_m \cdot \cos \omega t \cdot \sin \omega t \cdot \sin \varphi_1 \tag{6}$$

The remaining part in Eq. (4) is the harmonic power components. If the active power can be removed in Eq. (4), the remaining reactive and harmonic component power can be compensated with PAPF. Similarly, the reactive and harmonic current components are obtained by subtracting the real current from the total current given in Eq. (2). Therefore real current can be written as;

$$I_s(t) = I_m \sin(\omega t + \varphi_1) \tag{7}$$

Finally, by subtracting the actual current component from the total load current, the reference compensation current of the parallel active power filter given in Eq. (8) can be calculated;

$$I_c(t) = I_L(t) - I_s(t) \tag{8}$$

### 2.3 Hysteresis Band Current Control (HBCC)

Various current control methods have been applied to generate switching signals in active power filters [29]. In this paper, in order to obtain switching signals, HBCC

was used as a control method. It has been proven that HBCC is an effective technique to generate gate signals in all applications of active power filters that have voltage source inverters. Furthermore, this is a consistent and fast method that has a high accuracy rate [30]. HBCC is widely applied in APF for current harmonic compensation [31]. In HBCC as a control method, in order for generating switching signals, actual compensation current and reference compensation current are combined on a hysteresis band. With this non-linear current controlling technique, the continuous tracking of the output current of the inverter within a certain band is ensured [32].

In the block diagram given in Figure 9, the reference currents generated by SMT and the motor currents drawn from the grid are compared to be able to control the inverter current. The obtained current error is applied as input to the two-level hysteresis controller in order to generate switching signals. The block structure of the two-level hysteresis controller is shown in Figure 7. This block structure represents only one phase. Because the system is three-phase, three separate hysteresis controllers were used.

The current controller bandwidth is  $2\Delta I$ . The actual motor current ( $I$ ) varies in such a way that it stays within the  $\pm\Delta I$ -valued band around the reference currents ( $I_{ref}$ ). Therefore, in the actual motor current, the amount of deviation allowed in positive and negative directions is as much as the maximum  $I_{ref} \pm \Delta I$ . Controller outputs are digital outputs and take 0 and 1 values. If the controller output is 0, the S2 switching signal is generated and if the controller output is 1, the S1 switching signal is generated. The variations of S1 and S2 switching signals are shown in Figure 8.

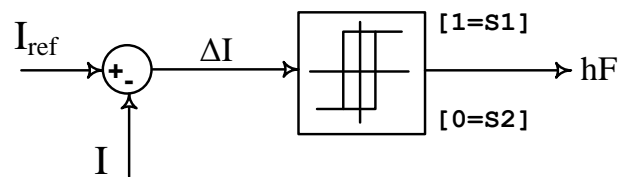


Figure 7. Hysteresis controller block diagram.

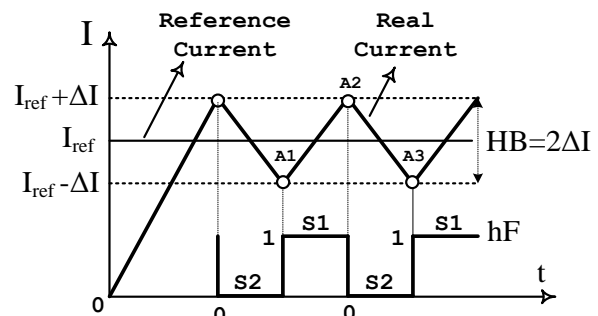


Figure 8. Structure of hysteresis band.

The  $I_{ref}-\Delta I$  value is the lower bound value of the hysteresis band and is shown in Figure 8 with the point A1. The A1 point is the lowest value where the actual motor current allowed by the controller can decrease. When it reaches to point A1, it is no longer allowed the actual motor current to decrease further, and at this point, the controller output becomes  $hF=1$  in order to produce the S1 switching signal that will increase the current. With the selection of the S1 switching signal at point A1, the actual motor current continues to increase with a positive slope up to point A2. The controller output at point A2 becomes  $hF=0$  and the S2 switching signal which will reduce the current is selected. Motor current continues to decrease with negative slope up to A3 point. In the hysteresis bandwidth determined in this way, switching signals that will allow the motor current to change in positive and negative directions are obtained. The current controller output according to the current error is mathematically expressed by Eq. (9).

$$hF = \begin{cases} 1 = S1 & I \leq I_{ref} - \Delta I \\ 0 = S2 & I \geq I_{ref} + \Delta I \end{cases} \quad (9)$$

Hysteresis bandwidth  $HB=2\Delta I$  directly affects the switching frequency of the inverter. Small bandwidth causes high switching frequency, while large bandwidth causes low switching frequency. Therefore, the switching frequency of the inverter should not be exceeded by

keeping the bandwidth at the optimum value. The switching frequencies obtained for 3 different hysteresis band values in the conducted simulation studies is given in Table 1 below.

### 3. Simulation Results

Figure 9 shows the Simulink block diagram for the entire system. In this simulation study, MATLAB/Simulink package program was utilized to perform the reactive power compensation of induction motor with PAPF. The source voltage and frequency were set to 311 volt and 50 Hz, respectively. DC-link voltage and coupling inductance were determined 311 V and 3 mH. Induction motor parameters were 4 kW for power, 400 V for voltage and 1430 rpm for speed.

The three-phase induction motor is supplied with a source voltage with a balanced 311 V amplitude. It is important that this voltage signal is pure sinusoidal because the unit sinusoidal signal used to create the reference current is derived from the source voltage.

Table 1. Switching frequency for different hysteresis bands.

Hysteresis Band (HB)	Switching Frequency ( $f_{sw}$ )
$2\Delta I = 1$	$f_{sw} = 5.082$ kHz
$2\Delta I = 0.5$	$f_{sw} = 7.342$ kHz
$2\Delta I = 0.1$	$f_{sw} = 12.540$ kHz

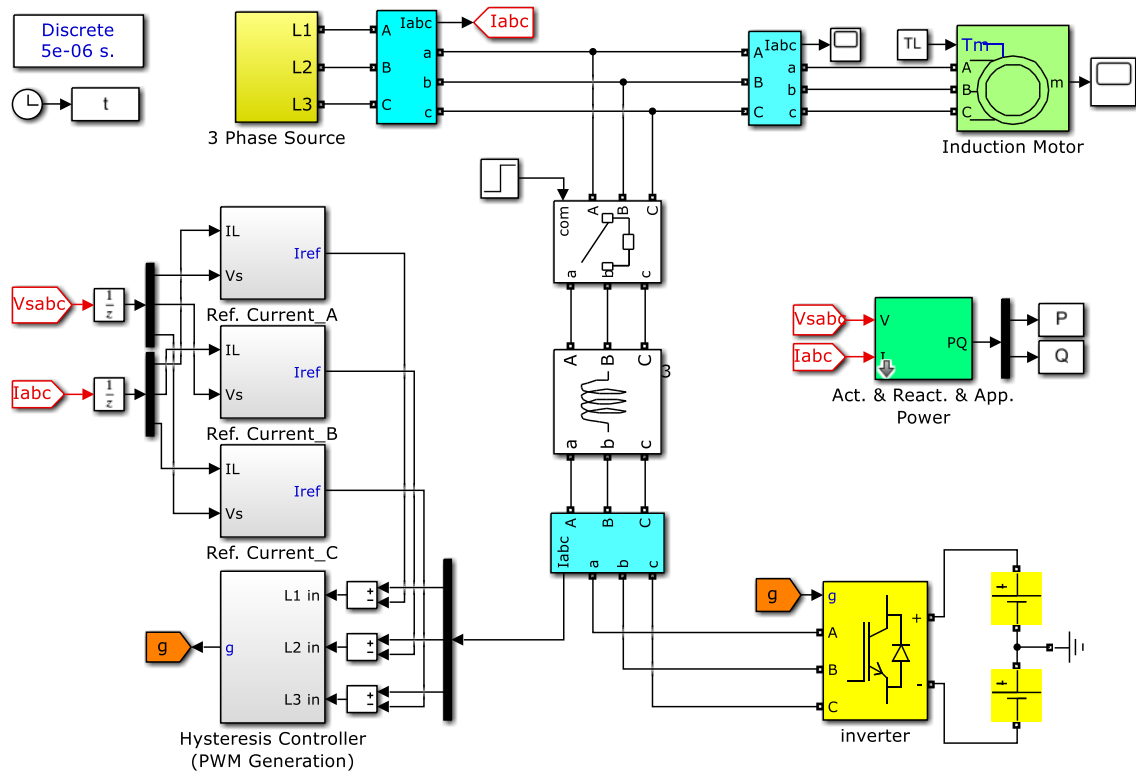


Figure 9. All system MATLAB/Simulink block diagram.

Figure 10 shows that there is a phase difference between voltage and current due to the reactive component before 0.16<sup>th</sup> of a second. In the same way, PAPF activates at 0.16<sup>th</sup> second. Therefore it makes reactive power compensation and eliminates the phase difference between the voltage and current.

Figure 11 shows that when PAPF enabled, the reactive power drawn from three-phase source by the induction motor is decreases to zero. In this way successful reactive power compensation is made. In terms of power signals, P, Q, and S refer to active, reactive, and apparent powers, respectively.

Figure 12 shows, motor power factor with filter and no filter at no-load conditions. After the filter is activated at 0.16<sup>th</sup> second than the power factor becomes 1.

The phase difference between current and voltage is

shown in Figure 13 when the induction motor is loaded with 2 Nm. At 0.16<sup>th</sup> second the PAPF is enabled. In this case, the phase difference observed between the voltage and the current disappears. Thus, PAPF successfully performs reactive power compensation even when the motor is loaded with 2 Nm.

Figure 14 shows that when PAPF is enabled, the reactive power drawn from the three-phase source by the induction motor decreases to zero. In this way, successful reactive power compensation is realized.

Figure 15 shows the motor power factor with filter and without filter at loaded conditions. After the filter is activated at 0.16<sup>th</sup> second, the PAPF performs a successful reactive power compensation by raising the power factor from 0.89 to 1.

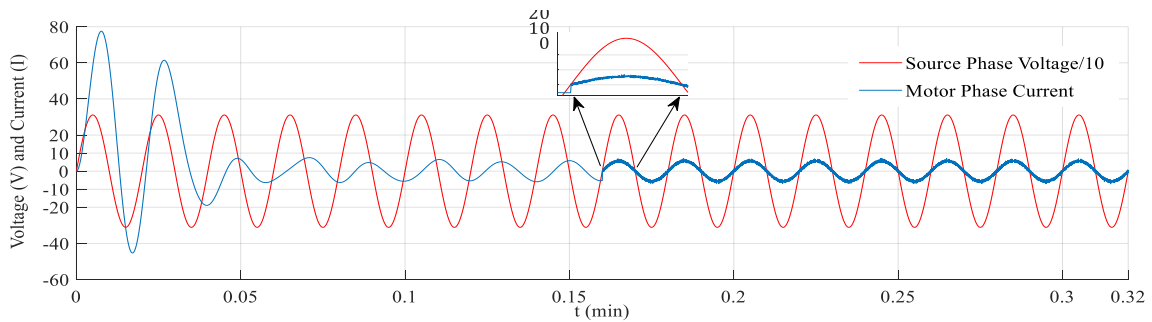


Figure 10. Source voltage and phase current of motor (no-load).

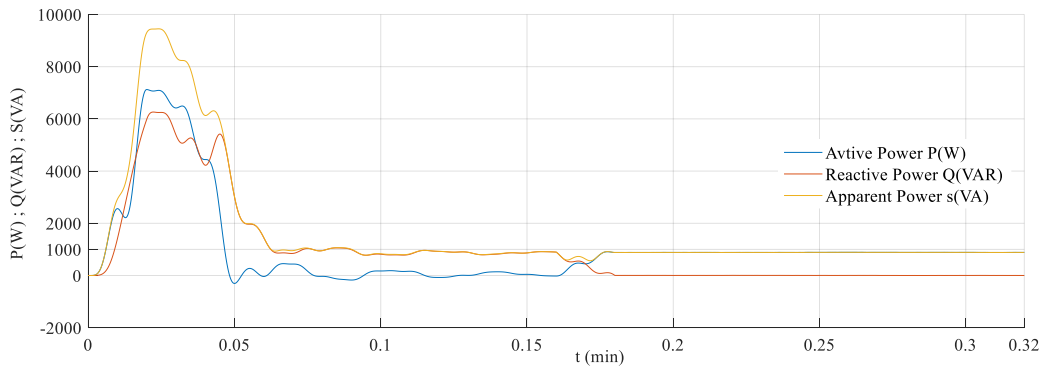


Figure 11. Active, reactive and apparent power signals.

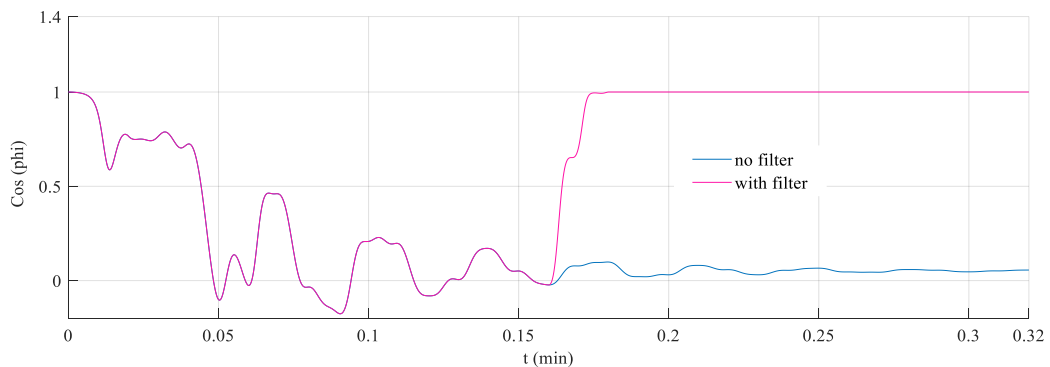


Figure 12. Power factor with filter and no filter at no-load conditions.

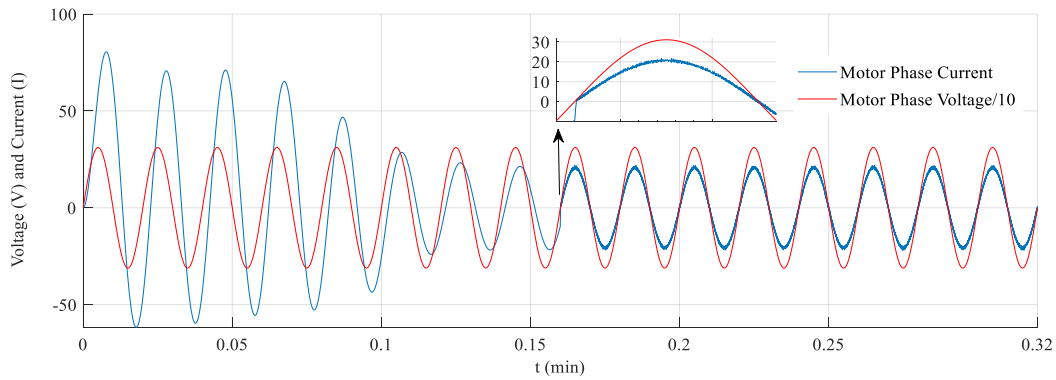


Figure 13. Source voltage and phase current of motor (loaded with 2 Nm).

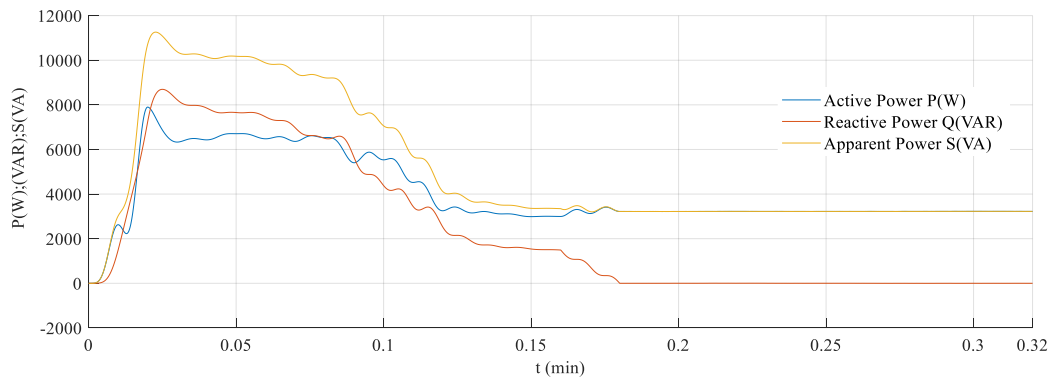


Figure 14. Active, reactive and apparent power signals (loaded with 2 Nm).

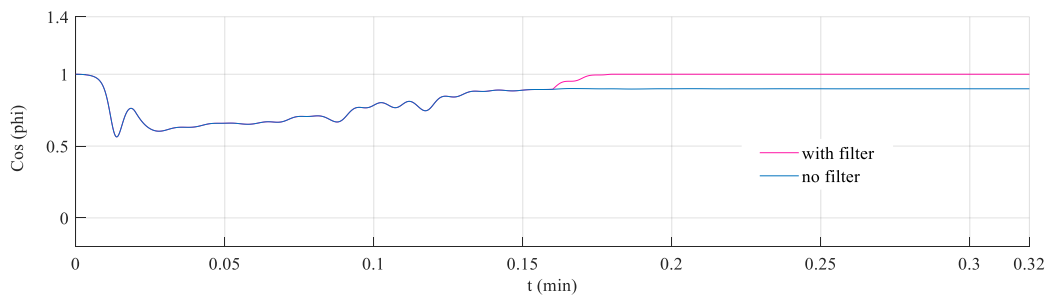


Figure 15. Power factor with filter and no filter at loaded conditions.

According to the block diagram given in Figure 9, the induction motor is directly connected to the 3-phase grid. There is no any switched power supply, such as inverter and converter, between the grid and the motor. Therefore, the current drawn from the grid by the motor running as an open loop is in pure sinusoidal form. However, there is a phase difference between the current drawn from the grid and the voltage. With the enabling of the Parallel Active Power Filter (PAPF), the motor draws the reactive energy, it needs, through the inverter connected to the DC bus. In this case, the phase difference between motor current and voltage becomes zero, but motor current loses its pure sinusoidal form. That is, it becomes a harmonic structure. Harmonics occur in all switched electronic circuits. The distortions to be caused by these harmonics vary according

to the switching frequency. In this respect, the total THD to occur in the current with the enabling of PAPF is found naturally higher than the situation before the compensation. This is because the currents drawn by the motor from the grid before compensation are pure sinusoidal and their THD is lower. In this respect, by considering that THD analysis of conditions before and after compensation could be a different study subject, no harmonic analysis was performed in this study.

#### 4. Conclusions

In the literature, there are different studies related to the reactive power compensation of the 3-phase induction motor with the parallel active power filter (PAPF). However, studies in which SMT, which is the reference current prediction



technique, and HBCC, which is the hysteresis controller structure, are used together have not been encountered much. In this study, in order to contribute to this area, a model in which the sine Multiplication Technique (SMT) and Hysteresis Band Current Controller (HBCC) structure were used together was created. With this model created in MATLAB/Simulink environment, reactive power compensation of a 3-phase induction motor was performed and the power factor was corrected. In this respect, this study is different from other studies that have been conducted and it partly contains originality.

Performance of a PAPF using the sine multiplication technique was investigated. Reference currents were estimated via sine multiplication technique. While the induction motor was running both no-load and loaded, the PAPF successfully performed reactive power compensation and power factor correction. Simulation studies were presented to evaluate the performance under different motor operating conditions. It was observed that PAPF performed a successfully reactive power compensation by increasing the power factor.

## Declaration

The author(s) declared no potential conflicts of interest with respect to the research, authorship, and/or publication of this article. The author(s) also declared that this article is original, was prepared in accordance with international publication and research ethics, and ethical committee permission or any special permission is not required.

## References

1. Yılmaz, Ö., Aksoy, M., Kesilmiş, Z. *Misalignment fault detection by wavelet analysis of vibration signals*. International Advanced Researches and Engineering Journal. 2019. 3(3), p.156-163.
2. Gundogdu, A., Dandil, B., Ata, F. *Direct Torque Control Based on Hysteresis Controller of Asynchronous Motor*. Science and Eng. J of Firat Univ. 2017. 29(1), p.197-205.
3. Ferreira, S.C., Gonzatti, R.B., Pereira, R.R., Silva, C.H., Silva, L. E. B., Torres, L.G. *Finite Control Set Model Predictive Control For Dynamic Reactive Power Compensation With Hybrid Active Power Filters*. IEEE Trans. On Industrial Electronics. 2018. 65(3),p.2608–2617.
4. Ye, J., Gooi, H.B., *Phase Angle Control Based Three-phase DVR with Power Factor Correction at Point of Common Coupling*. in Journal of Modern Power Systems and Clean Energy. 2020. 8(1), p. 179-186.
5. Roy, R.B., Cros,J., Basher, E., Akhter, S. *Power Compensation by DSTATCOM Plus SCESS*. Proceedings of the 2017 4th International Conference on Advances in Electrical Engineering (ICAEE). 2017. 28-30, p.100-108.
6. Wang, Y., Xu, Q., Chen, G. *Simplified Multi-Modular Shunt Active Power Filter System and its Modelling*. IET Power Electronic, 2015. 8(6), p. 967–976.
7. Cetin, S. *Power Factor Corrected and Fully Soft Switched PWM Boost Converter*. IEEE Transactions on Industry Applications, 2018. 54(4), p.3508–3517.
8. Badoni, M., Singh, A., Singh, B. *Adaptive Recursive Inverse-Based Control Algorithm for Shunt Active Power Filter*. IET Power Electronic, 2016. 9(5), p.1053–1064.
9. IEEE Std 519-1992. *Recommended Practices and Requirements for Harmonic Control in Electrical Power Systems*. IEEE Std, 1993. p.85-87.
10. Carlos, J., Gil, A., Pérez, E., Ariño, C., Beltran, H. *Optimization Algorithm for Selective Compensation in a Shunt Active Power Filter*. IEEE Transactions On Industrial Electronics, 2015. 62(6), p.3351–3361.
11. Fang, Y., Fei, J., Wang, T. *Adaptive Backstepping Fuzzy Neural Controller Based on Fuzzy Sliding Mode of Active Power Filter*.2020. doi:10.1109/ACCESS.2020.2995755, IEEE Access.
12. Sanam, J., Panda, A.K., Ganguly, Sanjib. *Optimal Phase Angle Injection for Reactive Power Compensation of Distribution Systems with the Allocation of Multiple Distribution STATCOM*. Arabian Journal for Science and Engineering, 2017. 42, p.2663–2671.
13. Ferreira, S.C., Gonzatti, R.B., Pereira, R.R., da Silva, C.H., da Silva, L.E.B., Lambert-Torres, G. *Finite Control Set Model Predictive Control for Dynamic Reactive Power Compensation With Hybrid Active Power Filters* in IEEE Transactions on Industrial Electronics. 2018. 65(3), p. 2608-2617.
14. Kandadai V., Sridharan, M., Parvathy, S.M., Pitchaimuthu, R., Kurup, D. *Performance Evaluation of FPGA-Controlled DSTATCOM for Load Compensation*. Arabian Journal for Science and Engineering, 2016. 41, p.3355–3367.
15. Komathi, C., Umamaheswari, M.G. *Erratum to Design of Gray Wolf Optimizer Algorithm-Based Fractional Order PI Controller for Power Factor Correction in SMPS Applications*. in IEEE Transactions on Power Electronics. 2020. 35(5), p.5543-5543.
16. Krama, A., Zellouma, L., Benaissa, A., Rabhi, B., Bouzidi, M., Benkhoris, M.F. *Design and Experimental Investigation of Predictive Direct Power Control of Three-Phase Shunt Active Filter with Space Vector Modulation using Anti-windup PI Controller Optimized by PSO*. Arabian Journal for Science and Engineering, <https://doi.org/10.1007/s13369-018-3611-6>.
17. Xu, Y., Yu, J., Cao, Y., Lu, X., Yu, J. *Double Resonant Output Filter to Eliminating the Tradeoff Between Bandwidth and Switching Ripple in Shunt Active Power Filters*. IET Power Electronics, 2016. 9(4), p.846–854.
18. Smith, I.J., Salmon, J. *High-Efficiency Operation of an Open-Ended Winding Induction Motor Using Constant Power Factor Control*. IEEE Transactions on Power Electronics. 2018. 33(12), p. 10663-10672.
19. Jibhakate, C.N., Chaudhari, M.A., Renge, M.M. *Reactive Power Compensation Using Induction Motor Driven by Nine Switch AC-DC-AC Converter*. IEEE Access. 2018. 6, p. 1312-1320.
20. Abu-Jalala, A.M., Cox, T., Gerada, C., Rashed, M., Hamiti, T., Brown, N. *Power Quality Improvement of Synchronous Generators Using an Active Power Filter*. IEEE Transactions on Industry Applications. 2018. 54(5), p. 4080-4090.

21. Durna, E. *Adaptive fuzzy hysteresis band current control for reducing switching losses of hybrid active power filter*. *IET Power Electronics*. 2018. 11(5), p. 937-944.
22. Zhang, H., Li, X., Xiao, S., Balog, R.S. *Hybrid hysteresis current control and low-frequency current harmonics mitigation based on proportional resonant in dc/ac inverter*. *IET Power Electronics*. 2018. 11(13), p. 2093-2101.
23. Diab, M., El-Habrouk, M., Abdelhamid, T. H., Deghedie, S. *Survey of Active Power Filters Configurations*. 2018 IEEE International Conference on System, Computation, Automation and Networking (ICSCA). Pondicherry, India, 2018. p.1-14.
24. Devassy, S., Singh, B. *Control of solar energy integrated active power filter in weak grid system*. 7th International Conference on Power Systems (ICPS), Pune. 2017. p. 573-578.
25. Yang, Z., Sun, J., Li, S., Huang, M., Zha, X., Tang, Y. *An Adaptive Carrier Frequency Optimization Method for Harmonic Energy Unbalance Minimization in a Cascaded H-Bridge-Based Active Power Filter*. *IEEE Transactions On Power Electronics*, 2018. 33(2), p.1024–1037.
26. Karaman, Ö.A., Erken, F., Cebeci, M. *Decreasing Harmonics via Three Phase Parallel Active Power Filter Using Online Adaptive Harmonic Injection Algorithm*. *Tehnički vjesnik*, 2018. 25(1), p.157-164.
27. Singh, B., AL-Haddad, K., Chandra, A. *A Review of Active Filters for Power Quality Improvement*. *IEEE Transaction on Industrial Electronics*, 1999. 46(5), p.133-138.
28. Terriche, Y., Golestan, S., Guerrero, J.M., Kerdoune, D., Vasquez, J.C. *Matrix Pencil Method-Based Reference Current Generation for Shunt Active Power Filters*. *IET Power Electronic*, 2018. 11(4), p.772-780.
29. Zhang, J., Yang, H., Wang, T., Li, L., Dorrell, D.G., Lu, D.D.C. *Field-Oriented Control Based on Hysteresis Band Current Controller for a Permanent Magnet Synchronous Motor Driven by a Direct Matrix Converter*. *IET Power Electronic*, 2018. 11(7), p.1277-1285.
30. Koya, S., Alsumiri, M. *A Modified Fuzzy Hysteresis Controller For Shunt Active Power Filter*. 2018 Renewable Energies, Power Systems & Green Inclusive Economy (REPS-GIE). Casablanca, Morocco, 2018. p.1-5.
31. Campanhol, L.B.G., Silva, S.A.O., Goedtel, A. *Application of Shunt Active Power Filter for Harmonic Reduction and Reactive Power Compensation in Three Phase Four-Wire Systems*. *IET Power Electronic*, 2014. 7(1), p.2825–2836.
32. Zhang, J., Li, L., Zhang, L., Dorrell, D. G. *Hysteresis Band Current Controller Based Field-Oriented Control for an Induction Motor Driven by a Direct Matrix Converter*. *IECON 2017-43rd Annual Conference of the IEEE Industrial Elect. Society*, Beijing, China, 2017. p.4633-4638.